

DE HAAS-VAN ALPHEN EFFECT IN ANTIMONY AT VERY LOW TEMPERATURES

N. B. BRANDT, N. Ya. MININA, and CHU CHEN-KANG

Moscow State University

Submitted to JETP editor February 23, 1966

J. Exptl. Theoret. Phys. (U.S.S.R.) **51**, 108–117 (July, 1966)

The angular dependences of the periods and the temperature dependences of the amplitudes of quantum oscillations in the magnetic susceptibility of antimony are investigated for the two principal crystal orientations at helium (4.2–1.5° K) and very low (0.08–0.1° K) temperatures in magnetic fields up to 19 kOe. A deviation of the equal-energy surface of antimony from an ellipsoidal shape is found which does not exceed 10% and agrees with results in ^[1]. The possible nature of the deviation is discussed. A pronounced deviation of the effective masses from proportionality to the respective extremal cross sections is noted which indicates that the electron and hole distributions are strongly nonquadratic.

INTRODUCTION

THE energy spectrum of Sb had not been clearly revealed up to now despite the numerous investigations of the subject. Considerable progress was achieved in ^[1-3], where it was indicated that the Fermi surface of antimony consists of three electron and six hole surfaces that resemble ellipsoids in first approximation. One of the short axes of the "ellipsoids" coincides with a binary axis direction, while the mean direction of the elongation forms angles of 4.4° and 34.2° with the basal plane for electrons and holes, respectively. The ellipsoids are brought into coincidence by a 120° rotation about the trigonal axis. The volume of the three electron ellipsoids equals the volume of the six hole ellipsoids. The electron and hole concentrations are $n_e = n_h = (5.36 \pm 0.06) \times 10^{19} \text{ cm}^{-3}$. All measurements for Sb were obtained at room, nitrogen, and helium temperatures.

Investigation of Bi has shown that additional information concerning the energy spectrum can be obtained at very low temperatures. ^[4] It was therefore of interest to investigate the de Haas-van Alphen effect in antimony at very low temperatures for comparison with ^[1, 2].

EXPERIMENTAL TECHNIQUE. SAMPLES

The anisotropy of magnetic susceptibility at very low temperatures was measured with the magnetic torsion balance described in ^[4]. An automatic device for compensating the moment of the forces acting on samples ^[5] enabled us to determine their orientation in a magnetic field H ,

and to register the oscillations of the magnetic moment M during a continuous variation of the magnetic field with an EP-2K two-coordinate automatic recorder. The x coordinate of this instrument was driven by the output emf of a Hall probe attached to one of the magnet poles. It was thus possible to sweep the x coordinate in the scale $1/H$, thereby considerably facilitating the problem of determining the oscillation period.

Temperatures of about 0.08° K were achieved through adiabatic demagnetization of ferric ammonium alum. Samples were warmed from $\sim 0.08^\circ$ to 0.1° K in 30–40 minutes, which was sufficient time to record two curves of $M(1/H)$, representing the field dependence of the magnetic moment.

Measurements were obtained for Sb samples, obtained by spark cutting from a bulk single crystal, in the form of $4 \times 4 \times 7$ -mm parallelepipeds having the required crystallographic orientation. The single crystals were grown by the Bridgman method from extra pure (99.9999%) antimony. Cooling from 300° to 4.2° K reduced the electrical resistance of the samples by a factor of 1500. The orientation of each single crystal was determined from the direction of its cleavage planes. The principal cleavage plane is perpendicular to the trigonal axis. Traces of secondary planes exhibit third-order symmetry in the basal plane and coincide with the directions of binary axes. The possible error in sample orientation was about 1°. After being annealed for four days at 300° C the samples were cooled gradually. The field of the electromagnet was calibrated by means of NMR and was determined with 0.3% accuracy.

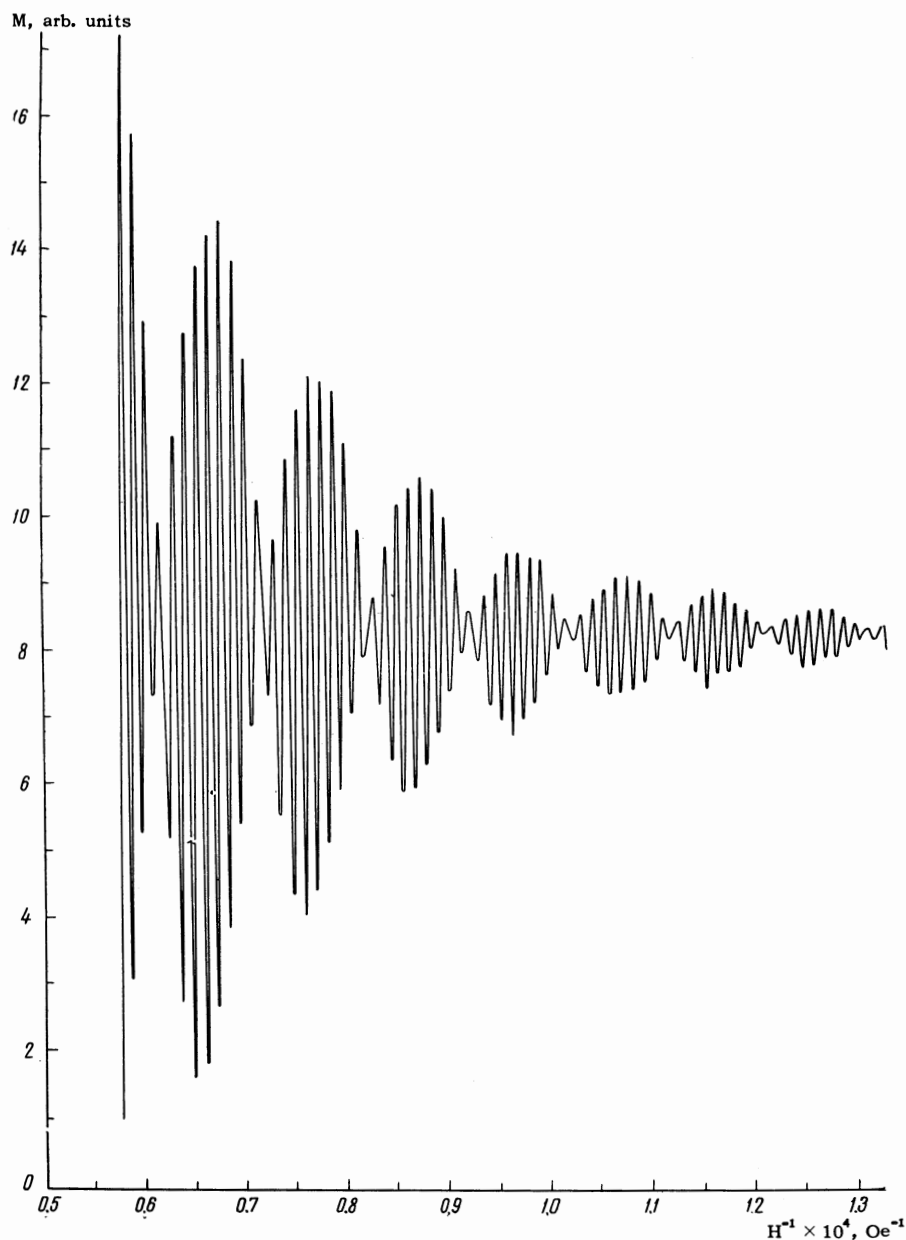


FIG. 1. Magnetic moment versus $1/H$ at 1.5°K for $\psi = 87.5^\circ$ in orientation II. Beats resulted from the superposition of two frequencies associated with two different cross sections of the hole "ellipsoids."

EXPERIMENTAL RESULTS

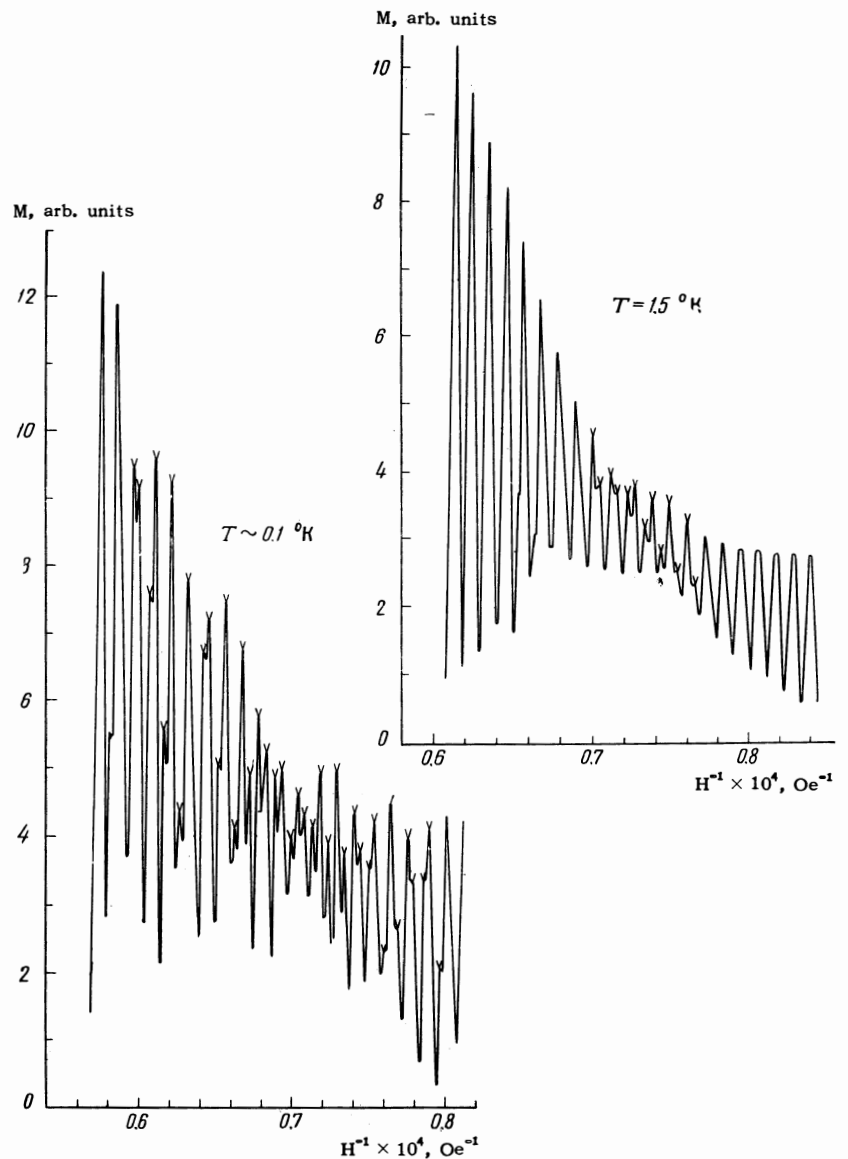
The quantum oscillations of magnetic susceptibility in Sb were investigated at 1.5° and $\sim 0.1^\circ\text{K}$ in magnetic fields up to 19 kOe for two orientations of the crystallographic axes. In the case of orientation I the binary axis was vertical, being parallel to the suspension axis of the sample; the field was varied in a plane passing through the trigonal and bisectrix axes. In orientation II the bisectrix axis was vertical; the field was measured in the plane of the trigonal and binary axes. The angle between the magnetic field direction and the trigonal axis will be denoted henceforth by ψ .

The energy spectrum of Sb is so complex that the experimental curves of $M(1/H)$ usually reveal

the superposition of two or more frequencies (Fig. 1) associated with different cross sections of the Fermi surface. The different field dependences of the amplitudes of the separate components enabled us to use beats in low fields for the purpose of determining some cross sections of the Fermi surface; other sections were determined from beats in high fields.

At very low temperatures the oscillation amplitudes were drastically augmented; the most important effect was the change of amplitude ratios in favor of the high-frequency components. Figure 2 demonstrates that it thus becomes possible to calculate reliably the oscillatory periods P associated with large cross sections of the Fermi surface. The accuracy of the periods was 1–2%,

FIG. 2. Relative increase in amplitudes of high-frequency oscillations, indicated by arrow heads, at very low temperature; $\psi = 155^\circ$ in orientation I.



depending on the complexity of the curves.

Although the very low temperature was considerably less efficient for Sb than for Bi, we were able to obtain a very much more complete picture of the angular dependence of the oscillatory period than at 1.5° K. Figures 3 and 4 show that for orientation I at the very low temperature we were able to investigate completely the minimum periods of "ellipsoid" A corresponding to the mean principal cross section of the hole "ellipsoid." For orientation II considerable progress was made into the region of large cross sections.

In Figs. 3 and 4 the experimental angular dependences of the oscillatory periods are compared with theoretical curves (dashed) that were calculated for the described ellipsoidal model using parameters taken from [1]. There is notably good agreement between our data for orientation I and

the experimental curves of [1] (solid curves in Fig. 3), which were obtained using a highly sensitive modulating technique. (Orientation II was not investigated in [1].)

Effective cyclotron masses were determined by studying the temperature dependence of the oscillation amplitudes. The temperature dependence of the amplitude of each separate component became available for investigation when the curves of the kind shown in Fig. 1 were decomposed graphically. The effective cyclotron masses were calculated from the equation

$$m_{S_m}^* = \frac{e\hbar}{c} \frac{\cosh^{-1}(\omega_{T_1}/\omega_{T_2})}{2\pi^2 k T_1} H, \quad (1)$$

where ω is the amplitude of oscillations, k is Boltzmann's constant, and $m_{S_m}^*$ is the cyclotron mass corresponding to the extremal cross section

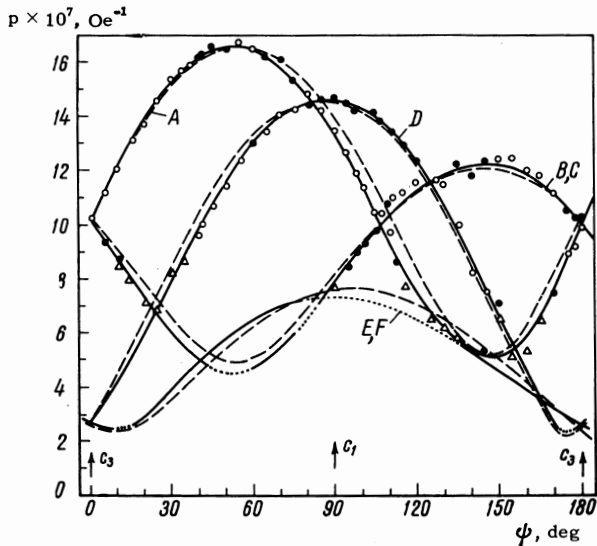


FIG. 3. Angular dependence of the magnetic susceptibility oscillation period in orientation I. \circ – fundamental period, \bullet – period derived from beats, \triangle – period observed at very low temperatures. The solid curves were plotted through the experimental points in [1]. The dashed curves represent calculations for the ellipsoidal model. Curves A, B, and C describe hole ellipsoids; curves D, E, and F describe electron ellipsoids. The trigonal and bisectrix axes are denoted by c_3 and c_1 , respectively.

S_m of the Fermi surface by a plane perpendicular to the magnetic field direction. For calculational convenience the amplitudes are compared at $T_2 = 2T_1 = 4.2^\circ \text{K}$. The average accuracy of the effective mass calculations is 3%. Table I gives values of $m_{S_m}^*$ determined for some angles ψ in orientations I and II.

DISCUSSION OF RESULTS

1. General remarks. In comparing our present results with those obtained by authors using a similar technique^[6, 7] it should be noted that at very low temperatures, even in conjunction with magnetic fields much lower than those used by Schoenberg^[6] and Saito,^[7] it became possible to obtain more complete information about the angular dependences of oscillatory periods and the extremal cross sections of the Fermi surface that are associated with the former through the equation $P = eh/cS_m$.

The advantage of the measurement of magnetic susceptibility using a torsion balance without modulating the magnetic field lies in the fact that we are thereby enabled to measure the absolute values of the oscillating part of the magnetic susceptibility, and can thus determine simultaneously the extremal cross sections and the corresponding effective cyclotron masses.

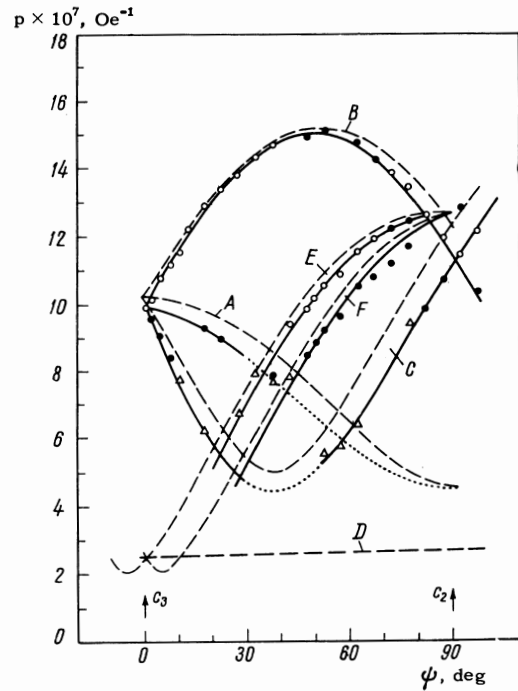


FIG. 4. Angular dependence of the magnetic susceptibility oscillation period in orientation II. \circ – fundamental period, \bullet – period derived from beats, ∇ – period observed at very low temperatures. The solid curves were plotted through the experimental points obtained in the present work. The dashed curves represent calculations for the ellipsoidal model. Curves A, B, and C pertain to hole ellipsoids; curves D, E, and F pertain to electron ellipsoids. The trigonal and binary axes are denoted by c_3 and c_2 , respectively.

The principal failing of this technique, which becomes especially evident when investigating materials such as Sb that possess a complicated energy spectrum, lies in the lack of any means for varying the amplitude ratios of the different oscillatory components. Therefore the full sensitivity

Table I

Orientation I			Orientation II		
ψ , deg	$\frac{m_{S_m}^*}{m_0}$	m^*/m_0	ψ , deg	$\frac{m_{S_m}^*}{m_0}$	m^*/m_0
Holes			Holes		
0	0.114	0.103	30	0.066	0.07
2.5	0.115	0.095	45	0.07	0.06
	0.111	0.101	54	0.074	0.06
17.5	0.093	0.078	Electrons		
	0.111	0.108	45	0.112	0.11
22.5	0.087	0.075	54	0.111	0.102
	0.137	0.11			
67.5	0.088	0.07			
87.5	0.106	0.08			
	0.111	—			
92	0.106	—			
	0.089	0.08			
Electrons					
67.5	0.103	0.110			

Note. The values of m^*/m_0 were taken from [2].

of the magnetic scale could not be utilized. The work was done with practically minimum sensitivity.

At very low temperatures the potentialities of torsion balance measurements are enhanced, because with decreasing temperature the amplitudes of the high-frequency components grow much more rapidly than those of the low-frequency components. However, since the anisotropy of the energy surfaces and effective masses is relatively small for antimony, at the very low temperatures the relative increase of the high-frequency amplitude was insufficient for a detailed investigation of large cross sections.

2. *Shape of the Fermi surface.* The angular dependences of the oscillation periods agree well with the model of the Sb Fermi surface proposed by Priestley. For convenience in analyzing, the shape of each surface will be considered in a coordinate system having its origin at the center of an ellipsoid. The axis p_1 is along the binary axis, the axis p_2 is in the direction of ellipsoidal elongation; p_3 is perpendicular to the other axes. The principal cross sections $p_2 = 0$, $p_3 = 0$, and $p_1 = 0$ of the ellipsoids will be denoted by S_1 , S_2 , and S_3 , respectively.

Although we obtained considerably less information about the angular dependences of extremal cross sections of the Fermi surface for orientation I than that obtained in ^[11], an analysis of our results for this orientation and for orientation II, which was not investigated in ^[11], permits several conclusions regarding the shape of the energy surface of Sb.

We must begin by noting that the angular dependence of an oscillatory period indicates an appreciable deviation of the Fermi surface from an ellipsoidal shape. The principal property of this deviation is the fact that the angle between the minimal and mean cross sections of the surface corresponding to curve A in Fig. 3 (i.e., between the two extremal periods on this curve) does not equal 90° . The real principal sections S'_1 and S'_2 are seen to form the angles 37° and 121° with the basal plane for holes, and 2° , 2.3° , and 94.5° for electrons; the data for electrons were obtained from ^[11]. Similar warping of the ellipsoids, leading to a shifting of the extremal periods, also appears for orientation II (curve B).

In calculating the theoretical curves for the ellipsoidal model that are shown in Figs. 3 and 4 the angle between the ellipsoids and the basal plane was measured from the mean direction of elongation: 34.2° for holes and 4.4° for electrons.

Figure 3 shows that cross sections of real energy surfaces intermediate between the principal ones exceed the analogous sections of the corresponding ellipsoids. This difference is especially clear for orientation II (Fig. 4). This orientation is characterized by angular dependences of intermediate cross sections that must deviate most drastically from ellipsoidal character, because the principal cross sections S_1 , S_2 , and S_3 for the ellipsoidal model were taken to equal the principal sections S'_1 , S_2 , and S'_3 of a real surface. All experimentally observed intermediate sections are considerably larger than the corresponding sections of an ellipsoid (for example, curves A, E, F, and C in Fig. 4). However, Fig. 4 shows that the maximum deviation from the ellipsoidal model does not exceed 10%. It is of interest that in the region of minimal cross sections (the upper part of curve B in Fig. 4) the deviation from the ellipsoidal model is small.

We have found that the overall picture of the warping of electron and hole surfaces can be represented as a transition from ellipsoids to ovaloids which are at the same time warped unsymmetrically relative to a plane passing through p_1 and p_2 (S_2). The resulting surface is characterized by the cross sections $p_1 = 0$ represented in Fig. 5, where the dashed curves denote the corresponding sections of the initial ellipsoids. The possibility that this kind of warping occurs for the electron surfaces of metals such as bismuth was predicted by Abrikosov and by Fal'kovskii.^[8] It is interesting that the hole and electron surfaces are warped in different directions relative to the plane $p_3 = 0$.

Since the angular dependences of the oscillatory periods are symmetric relative to their extremal values when the field is parallel to the basal plane,^[11] we can assume C_{2h} symmetry for the electron and hole surfaces. Figure 6 shows a possible arrangement of the surfaces in the Brillouin zone that is in accord with the calculated band structure of group V semimetals.^[9, 10]

3. Some comments regarding electron and hole dispersion in Sb. A nonquadratic law of current carrier dispersion in antimony is indicated, first of all, by the nonellipsoidal shapes of the electron and hole surfaces. As already mentioned, the deviation from ellipsoidal shapes for Sb is at most 10%. However this does not mean that the departure from the quadratic law is of equal relative smallness.

We know that in the case of a quadratic dispersion law the extremal cross sectional areas of the Fermi surface are proportional to the effective

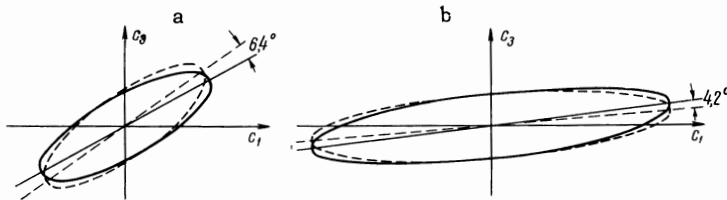


FIG. 5. The most probable shapes of the sections of (a) hole and (b) electron energy surfaces by the plane $p_1 = 0$. Each dashed curve denotes the cross section of the initial ellipsoid. When the minimal sections coincide the elongated direction of a real surface departs from the direction of the maximal principal axis of the ellipsoid. The trigonal and bisectrix axes are denoted by c_3 and c_1 , respectively.

cyclotron masses. Therefore the difference between the ratios of the cross sections and of the corresponding masses serves as a criterion of the departure from a quadratic law. It is therefore of interest to compare the ratio of extremal Fermi-surface sections for Sb with the corresponding ratio of the extremal cyclotron masses m^* obtained in [2]. From this comparison, which is represented in Table II, we draw the following conclusions:

a) The cyclotron masses m^* are not proportional to the corresponding cross sections.

b) The largest deviation from proportionality occurs in the case of S_2/S_1 and comprises 33% and 75% for holes and electrons, respectively.

c) The maximum lack of correspondence between S_i/S_k and m_i^*/m_k^* is observed for electron surfaces which appear to have more nearly ellipsoidal shapes than the hole surfaces.

The drastic discrepancy between S_i/S_k and m_i^*/m_k^* indicates that the electron distribution $\epsilon(p)$ in antimony is strongly non-quadratic. We therefore obtain an inaccurate value of the energy limit E_0 when we use the conventional formula

$$E_0 = S_m/2\pi m_s^*,$$

which is valid only for a quadratic distribution. The values of E_0 computed by this means [(16.3 \pm 0.7) $\times 10^{-14}$ erg for holes and (15.2 \pm 0.5) $\times 10^{-14}$ erg for electrons] must therefore be regarded as only approximate values.

Table I shows that the discrepancy between the masses $m_{S_m}^*$ and the cyclotron masses m^* [2] can amount to as much as 25%; this considerably ex-

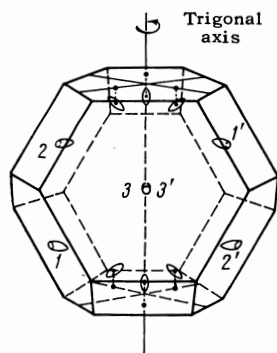


FIG. 6. Possible arrangement of the equal-energy surfaces of antimony in the reduced Brillouin zone. Halves of the electron surfaces are designated by numerals. The signs of the inclination angles of the surfaces agree with [1]. The electron surfaces are located at the centers of pseudo-hexagonal faces; the hole surfaces are inside the zone.

Table II

Quantity	Holes	Electrons	Quantity	Holes	Electrons
S_1 , at. units	1.61	1.82	m_1^*/m_0	0.058	0.09
S_2 , at. units	5.19	11.5	m_2^*/m_0	0.25	0.325
S_3 , at. units	5.7	9.62	m_3^*/m_0	0.215	0.315
S_3/S_1	3.54	5.28	m_3^*/m_1^*	3.7	3.5
S_3/S_2	1.1	0.83	m_3^*/m_2^*	0.86	0.97
S_2/S_1	3.23	6.3	m_2^*/m_1^*	4.3	3.67

ceeds the accuracy with which $m_{S_m}^*$ is calculated from experimental curves. The values of $m_{S_m}^*$ usually exceed the corresponding values of m^* .

We are deeply indebted to A. I. Shal'nikov and Yu. P. Gaïduk for their interest in this work.

¹ L. R. Windmiller and M. G. Priestley, *Solid State Comm.* **3**, 199 (1965).

² W. R. Datars and J. Vanderkooy, *IBM J. Res. Develop.* **8**, 247 (1964).

³ Y. Ishizawa and S. Tanuma, *J. Phys. Soc. Japan* **20**, 1278 (1965).

⁴ N. B. Brandt, T. F. Dolgolenko, and N. N. Stupochenko, *JETP* **45**, 1319 (1963), *Soviet Phys. JETP* **18**, 908 (1964).

⁵ N. B. Brandt and Ya. G. Ponomarev, *PTÉ* **6**, 114 (1961).

⁶ D. Shoenberg, *Phil. Trans. Roy. Soc. (London)* **A245**, 1 (1952).

⁷ Y. Saito, *J. Phys. Soc. Japan* **19**, 1319 (1964).

⁸ L. A. Fal'kovskii, Candidate dissertation, *Inst. Phys. Prob.*, 1963.

⁹ M. H. Cohen, L. M. Falicov, and S. Golin, *IBM J. Res. Develop.* **8**, 215 (1964).

¹⁰ L. M. Falicov and S. Golin, *Phys. Rev.* **137**, A871 (1965).